


**Prigogine-Defay ratio of glassy freezing scales with liquid fragility**A. Loidl<sup>1,\*</sup>, P. Lunkenheimer<sup>1</sup> and K. Samwer<sup>2</sup><sup>1</sup>*Experimental Physics V, University of Augsburg, 86135 Augsburg, Germany*<sup>2</sup>*I. Physikalisches Institut, University of Göttingen, Göttingen, Germany* (Received 19 April 2024; revised 26 February 2025; accepted 3 March 2025; published 18 March 2025)

A detailed study of published experimental data for a variety of materials on the incremental variation of heat capacity, thermal expansion, and compressibility at glassy freezing reveals a striking dependence of the Prigogine-Defay ratio  $R$  on the fragility index  $m$ . At high  $m$ ,  $R$  approaches values of  $\sim 1$ , the Ehrenfest expectation for second-order continuous phase transitions, while  $R$  reaches values  $> 20$  for low fragilities. We explain this correlation by the degree of separation of the glassy freezing temperature from a hidden phase transition into an ideal low-temperature glass.

DOI: [10.1103/PhysRevE.111.035407](https://doi.org/10.1103/PhysRevE.111.035407)**I. INTRODUCTION**

The glass transition as a function of temperature or pressure is the continuous solidification of a supercooled liquid avoiding crystallization. It occurs in a large variety of materials of high technological importance, ranging from silicate glasses, amorphous metals, and ionic salts to polymers. Despite considerable experimental and theoretical progress, its microscopic understanding remains a controversially discussed problem. The glass-transition temperature  $T_g$  is not a critical temperature, but it marks a kinetic arrest below which amorphous materials are too viscous to flow on experimentally accessible timescales [1–8]. The remarkable features related to glassy freezing were explained by different concepts, which can be grouped [1] into theories assuming an underlying phase transition into an “ideal” equilibrium glass state, either at  $T_c < T_g$  [9–14] or at  $T_c > T_g$  [15–18], and models describing glassy freezing as a purely kinetic process [19–22]. Very recently, utilizing molecular-dynamics simulations, it has been documented that glass transitions into amorphous phases might be even more complex [23,24].

In the present work, we adapt the view of models assuming a critical temperature  $T_c$ , marking a hidden phase transition, which cannot be reached because of the freezing-in of structural dynamics at  $T_g$ . Such ideas started with Kauzmann’s proposal [25] of an entropy catastrophe, where an extrapolation of the experimentally determined entropy of the supercooled liquid falls below that of the crystal at a temperature, nowadays called Kauzmann temperature  $T_K$ . Notably, critical remarks and questions concerning the validity of the Kauzmann paradox were raised in Refs. [26,27]. However, more recent Monte Carlo simulations show that the configurational entropy is tending strongly towards zero as systems are equilibrated at temperatures significantly below  $T_g$  [28,29], which is consistent with a phase transition to an ideal glass state at  $T_K$ . Similar conclusions can be drawn from vapor-deposition experiments on ultrastable glasses [30].

An adequate way to describe the typical super-Arrhenius behavior of relaxation time  $\tau$  (or viscosity  $\eta \propto \tau$ ) of supercooled liquids is the Vogel-Fulcher-Tammann (VFT) law:  $\tau = \tau_0 \exp[D T_{VF}/(T - T_{VF})]$  [1,31–36]. Here  $\tau_0$  corresponds to an inverse attempt frequency, and  $D$  is the strength parameter quantifying the degree of deviations from pure Arrhenius behavior [34].  $T_{VF}$  is the Vogel-Fulcher temperature, where  $\eta$  or  $\tau$  are predicted to diverge. Often, the ratio  $T_K/T_{VF}$  is found to be close to unity [5,37,38] (see Appendix A for a discussion of deviations found in certain materials) and, in the following, we will use  $T_{VF}$  to estimate the ideal glass-transition temperature. The VFT law can be rationalized using the Adam-Gibbs theory [10], which assumes that supercooled liquids comprise cooperatively rearranging regions whose growth on decreasing temperature leads to a concomitant growth of the apparent activation energy governing structural relaxations. These ideas were further developed in the random first-order phase-transition theory [11,12]. Indeed, in a series of experimental and theoretical works it was shown that the super-Arrhenius behavior of many glass-forming liquids is due to growing lengthscales, which can be directly measured via higher-order susceptibilities [39–43]. A more detailed discussion, including possible shortcomings of the VFT law and treating the influence of different fitted temperature regimes on the VFT parameters, is given in the Appendix A, including Fig. 3.

The glass-transition temperature is usually defined by an anomaly in the specific heat, measured with a cooling rate of 10–20 K/min, or by the temperature at which the relaxation time reaches a value of  $\sim 100$  s or the viscosity  $\sim 10^{13}$  Poise. The glass transition is a kinetic phenomenon, hence  $T_g$  depends on the cooling rate. As indicated in Fig. 4 and explained in more detail in Appendix B, it is visible by a change in the temperature dependence of volume  $V$  or entropy  $S$ , without any latent heat contributions. At the coexistence line (see the inset of Fig. 4), the entropy and volume in the two phases are identical, but discontinuities appear in the second derivatives of the Gibbs free energy, such as the heat capacity, thermal expansion, or compressibility. In this respect, glassy freezing resembles a second-order phase transition, and one may ask

\*Contact author: [alois.loidl@physik.uni-augsburg.de](mailto:alois.loidl@physik.uni-augsburg.de)

whether the Ehrenfest relations characterizing such continuous transitions are applicable. Ehrenfest has shown that, for the inverse pressure dependence of the critical temperature  $T_c$ , the following two equations must be valid [44]:

$$dp/dT_c = \Delta c_p / T_c V_c \Delta \alpha_p \equiv A, \quad (1)$$

$$dp/dT_c = \Delta \alpha_p / \Delta \kappa_T \equiv B. \quad (2)$$

Here  $V_c$  is the specific volume at  $T_c$ , while  $\Delta c_p$ ,  $\Delta \alpha_p$ , and  $\Delta \kappa_T$  are the discontinuities in heat capacity, thermal expansion, and compressibility, respectively, when crossing the phase boundary.  $A$  and  $B$  denote the right-hand terms in these equations, discussed later. Equation (1) is derived from an isobaric path across the phase transition, assuming the continuity of entropy at  $T_c$ , while Eq. (2) follows from an isothermal path, assuming continuity of the volume. Prigogine and Defay [45] concluded that similar relations, leading to

$$R = \frac{\Delta c_p \Delta \kappa_T}{V_g T_g (\Delta \alpha_p)^2} = 1, \quad (3)$$

(assuming  $A = B$ ), should also apply to the glass transition, where  $V_g$ ,  $\Delta c_p$ ,  $\Delta \alpha_p$ , and  $\Delta \kappa_T$  are the corresponding quantities at  $T_g$ .  $R$  nowadays is called the Prigogine-Defay ratio (PDR).

The analysis of experimental data on the validity of Eq. (3) revealed that Eq. (1) (with  $T_c = T_g$  and  $V_c = V_g$ ) is correct and holds for most of the glass-forming materials studied, while Eq. (2) is often invalid, resulting in  $R \geq 1$  [46–52]. The violation of Eq. (3) in glasses was explained assuming that more than one order parameter has to be taken into account [46–49,53]. Several critical remarks on this interpretation and alternative explanations were proposed [54–61]. Reference [56] elucidates how configurational entropy enters the PDR. Moreover, the authors of Ref. [61] pointed out that glassy freezing is a kinetic process, and they argued that the quantities determining  $R$  may be history-dependent. However, one should note that most experiments were done with conventional cooling rates (order K/min), without exotic histories. Moreover,  $\Delta \alpha$  essentially is not history-dependent (see, e.g., Fig. 4 in Appendix B) and  $\Delta \kappa$  is not very sensitive at all to the glass transition. Furthermore, assuming reasonable rate variations,  $T_g$  is only weakly rate-dependent, as is the volume. Of course,  $\Delta c$  is history-dependent, but as mentioned above, it is mostly measured in similar ways with conventional heating and cooling rates of the order of 10 K/min. Possible errors of the measured quantities due to these facts are well within the scatter of the data points, mainly arising from investigations of materials with different grades of purities, different measuring techniques and evaluation methods, and partly from experiments under extreme conditions.

Guided by a detailed study of published results, in the further course of this work we demonstrate that so-called strong liquids show strong deviations of the PDR from unity, while so-called fragile liquids reveal values close to 1. This leads to a completely new route towards the interpretation of the PDR in glasses: We propose that the degree of separation of the glass-transition temperature from that of the extrapolated critical behavior plays a fundamental role for the deviation of the PDR from unity predicted for thermodynamic second-order phase transitions. To check the validity of this assumption, it is important to provide a reliable measure of this separation, and

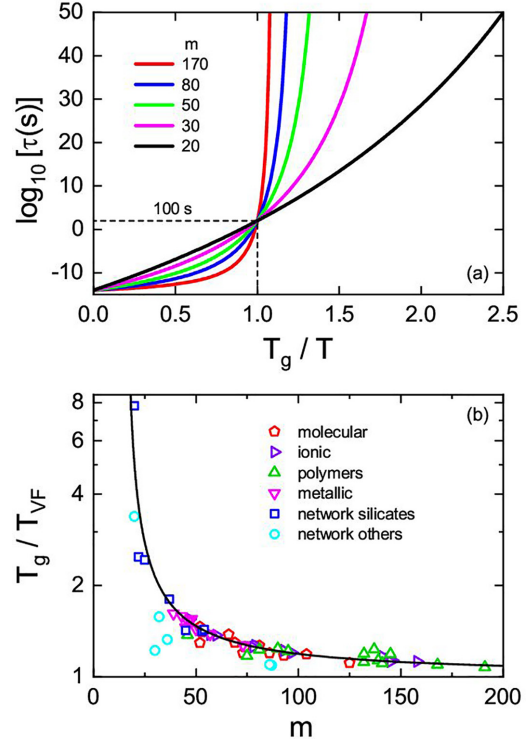


FIG. 1. (a)  $T_g$ -normalized Arrhenius representation (Angell plot [63]) of the temperature-dependent relaxation times of supercooled liquids for fragilities  $m$  between 20 and 170, calculated assuming VFT behavior. (b) Fragility dependence of the ratio of glass-transition and Vogel-Fulcher temperature. The symbols show experimental results derived for a variety of materials belonging to different classes of glass formers, and the line was calculated from the VFT equation (see the text for details). The characteristic temperatures and fragilities of all materials are documented in Appendix C in Table I.

in the following we calculate the ratio of  $T_g/T_{VF}$  to validate this assumption.

## II. SEPARATION OF A POSSIBLE PHASE TRANSITION FROM GLASSY FREEZING

Within the strong-fragile classification scheme of glasses as introduced by Angell [34], the fragility index  $m$  is commonly used to quantify the deviations of  $\tau(T)$  from Arrhenius behavior. It is defined [62] by the slope at  $T_g$  in an Angell plot [63],  $\log_{10}(\tau)$  versus  $T_g/T$ , and related to the strength parameter in the VFT equation via  $m = 16 + 590/D$  [62]. Interestingly, this quantity can also be regarded as a measure of how close the laboratory glass-transition temperature approaches the critical Vogel-Fulcher temperature,  $T_{VF}$ . This is visualized in Fig. 1(a) showing an Angell plot extending to temperatures far below the glass-transition temperature. For high fragilities, the divergence temperature,  $T_{VF}$ , comes close to  $T_g$ , while for strong glass formers it is shifted to much lower temperatures. Assuming  $\tau(T_g) = 100$  s and  $\tau_0 = 10^{-14}$  s [62], the fragility dependence of the ratio  $T_g/T_{VF}$  can be estimated as  $T_g/T_{VF} = m/(m-16)$ , which is indicated as a solid line in Fig. 1(b). In strong glasses with  $m$  approaching

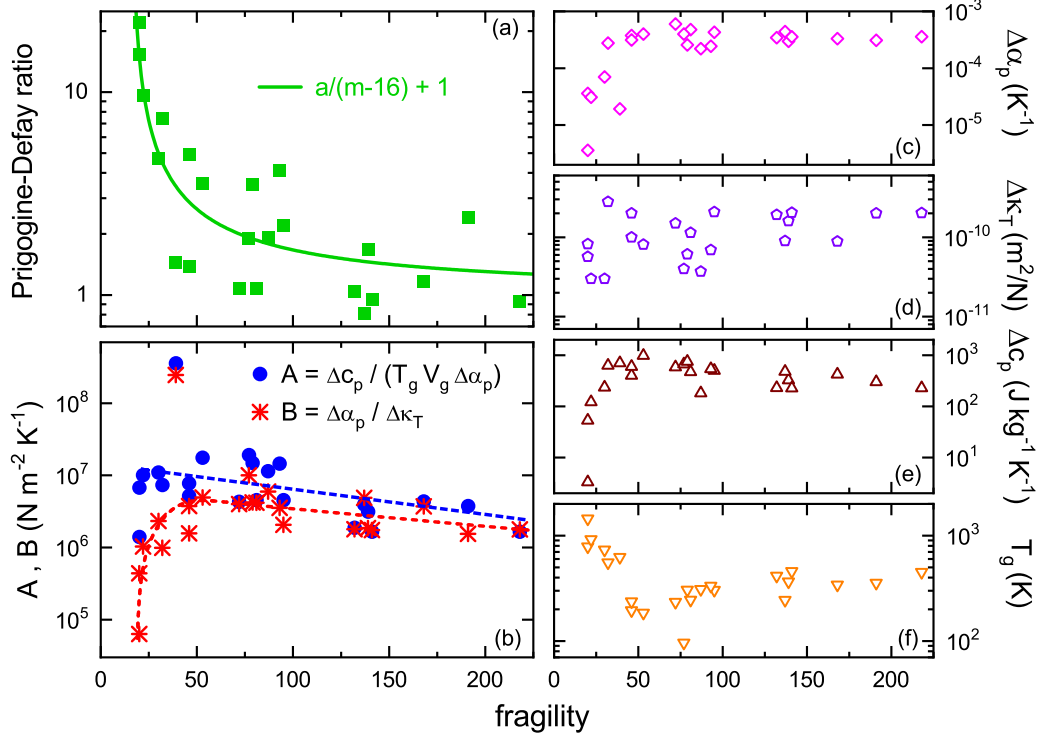


FIG. 2. (a) Prigogine-Defay ratio  $R$  as a function of fragility  $m$  for various glass-formers as listed in Table II of Appendix D. The line is a fit by the indicated formula, leading to  $a \approx 56$ . (b) Temperature dependence of  $A$  and  $B$ , the right-hand quantities in the Ehrenfest equations [Eqs. (1) and (2)]. The dashed lines are drawn to guide the eye. (c)–(e) Fragility dependences of the incremental variations of thermal expansion  $\Delta \alpha_p$ , compressibility  $\Delta \kappa_T$ , and heat capacity  $\Delta c_p$  at the glass transition. In (d), we excluded the value of the metallic glass, which is three orders of magnitude lower. (f)  $m$  dependence of the glass-transition temperature  $T_g$ . All numerical data for this figure are listed in Table II of Appendix D.

16, corresponding to plain Arrhenius behavior ( $T_{VF} = 0$  K), this ratio diverges, while for large fragilities it approaches unity, leading to  $T_g \approx T_{VF}$ . Overall, for fragility values between 20 and 190, the ratio decreases by almost a factor of 5. Finally, objections concerning the criticism for continuing the VFT law for temperatures below glassy freezing are summarized in Appendix A. In Fig. 1(b), we compare the theoretical prediction (line) with experimental results, revealing a reasonable agreement. The involved quantities, discussed in Appendix C and listed in Table I, were deduced for vastly different material classes from fits of  $\tau(T)$  or  $\eta(T)$  (giving  $T_{VF}$ ,  $m$ , and  $T_g$ ), from the corresponding Angell plots ( $m$ ), and/or from heat-capacity measurements ( $T_g$ ). We conclude that in fragile glass formers,  $T_g$  approaches  $T_{VF}$ , while in strong glass formers, these two characteristic temperatures are widely separated. Consequently, the Ehrenfest relations can be expected to approximately hold for fragile glasses, where the relevant quantities are measured close to the phase boundary. In strong glasses, the measurements are performed at  $T_g \gg T_{VF}$ , too distant from the ideal glass transition to allow for a reliable determination of the PDR.

### III. FRAGILITY DEPENDENCE OF THE PDR

In the following, we relate the fragilities, which can be regarded as a measure of separation of glass-transition and estimated critical temperatures (Fig. 1), to the published results of the PDR in a variety of glass-forming systems. In Appendix D

in Table II, we have collected all available relevant data for a variety of glass-forming materials, for which thermal expansion, heat capacity, and compressibility were measured above and below the glass transition, and where, in addition, the specific volume at  $T_g$  and the fragility were reported. We have critically reviewed existing tables [47,50,53,57,58,64,65]; however, we always tried to refer to the original literature, and, in the case of multiple experiments, to select the best documented results (see Appendix D for details). These data allow calculating the PDR [Eq. (3)] and the two quantities  $A$  and  $B$  [Eqs. (1) and (2)] for various classes of amorphous materials spanning a wide range of fragilities.

Figure 2(a) shows the experimental findings from Table II (Appendix D) for the PDR  $R$  as a function of fragility  $m$ . Even though there is considerable scatter, it reveals a continuous increase of  $R$  on decreasing fragility, spanning  $R$  values from close to 1 at high, to  $\sim 20$  at low fragilities. The scatter of  $R$  can be expected considering the variety of applied techniques and the experimental difficulties, partly under extreme conditions, to determine the incremental values of the thermodynamic and mechanical quantities in the liquid and solid phases crossing the glass transition. A more detailed analysis of the statistical scatter of data points in Fig. 2(a) and arguments that the found  $R(m)$  correlation indeed does exist are presented in Appendix E. Notably, we provide a PDR value for amorphous silica, where no thermal expansion coefficient is reported for the supercooled liquid, by assuming the found universality  $\alpha_l = 3 \alpha_g$ , where  $\alpha_l$  and  $\alpha_g$  are the thermal expansion

coefficients in the liquid and glass state, respectively [66]. The line in Fig. 2(a) is a fit by the empirical formula  $R = a/(m - 16) + 1$ , with a single fit parameter  $a \approx 56$ , supposing a divergence of  $R$  at  $m = 16$  and  $R \approx 1$  for high fragilities, the value expected for a second-order phase transition. This fit should not be overinterpreted; it is purely phenomenological and assumes an asymptotic approach of  $R = 1$  for  $m \rightarrow \infty$ . While it reasonably describes the experimentally observed  $R(m)$  evolution, the data are also consistent with  $R$  already reaching  $\sim 1$  for  $m > 100$ .

It should be possible to trace back the found universal correlation of  $R(m)$  and the deviations of  $R$  from unity to the two quantities  $A$  and  $B$  defined in the Ehrenfest relations, Eqs. (1) and (2). As pointed out above, the first equation is valid if the configurational entropy, and the second if the volume, determines  $T_g$  [48]. In an ideal second-order phase transition,  $A = B$  must hold, resulting in  $R = 1$ . Considering the available experimental pressure dependence of the glass transition, Eq. (1) holds for most glasses, while  $B$  defined in Eq. (2) is always too low [50]. In Fig. 2(b), we show the fragility dependences of  $A$  and  $B$ . We find a gradual increase of  $A$  on decreasing  $m$  (circles) and, except for the lowest  $m$  values, a similar gradual increase of  $B$  (stars). Notably,  $B$  is always smaller than  $A$ , leading to  $R > 1$  in agreement with Fig. 2(a). However, for the lowest fragilities,  $m < 35$ , Fig. 2(b) reveals a strong decrease of  $B$ , resulting in strongly increasing PDRs in Fig. 2(a). On the contrary, for large  $m$ ,  $A$  and  $B$  approach each other, suggesting  $R \approx 1$  as expected for second-order phase transitions in the sense of Ehrenfest. Specifically, the strong decrease of  $B$  for  $m < 35$  [Fig. 1(b)], with a concomitant strong increase of  $R$  [Fig. 2(a)], shows a striking correlation with the increase of  $T_g/T_{VF}$  at low  $m$  [Fig. 1(b)], pointing towards a fundamental microscopic origin.

For a better insight into the fragility dependence of  $R$ , it is important to consider the  $m$  dependences of all quantities entering the PDR [Eq. (3)], which are documented in Figs. 2(c)–2(f). We do not plot  $V_g(m)$ , which is rather constant with values mostly ranging from  $\sim 0.5$  to  $1 \times 10^{-3}$  m<sup>3</sup>/kg (see Table II in Appendix D). On decreasing  $m$ , the increment of thermal expansion  $\Delta\alpha_p$  (c) is constant, while  $\Delta c_p$  (e) reveals a small increase, but both exhibit significant downturns of approximately two orders of magnitude for the lowest fragilities. The increment of isothermal compressibility  $\Delta\kappa_T$  [Fig. 2(d)] appears rather independent of  $m$  when considering the data scattering. Finally,  $T_g(m)$  is presented in Fig. 2(f). On decreasing fragility, it shows a small continuous decrease, followed by a strong increase at the lowest  $m$  values. These detailed  $m$  dependences cause the behavior of  $A(m)$  and  $B(m)$  and, consequently, the fragility dependence of  $R(m)$ . Concerning the quantity  $A$  in the first Ehrenfest relation [Eq. (1)], the fragility dependences of  $\Delta\alpha_p$ ,  $\Delta c_p$ , and  $T_g$  almost compensate, yielding a weak, continuous evolution as a function of fragility.  $B$  in the second Ehrenfest relation [Eq. (2)] essentially mirrors the fragility dependence of  $\Delta\alpha_p$ , because  $\Delta\kappa_T$  remains constant within experimental uncertainty. The low values of the incremental changes of heat capacity and thermal expansivity mostly occur in network-forming oxide glasses (see Table II in Appendix D). It should be noted that there are ideas [67,68] that such strong inorganic networks may undergo an order-disorder-type liquid-liquid phase transition at

much higher temperatures, thereby reducing configurational entropy considerably.

#### IV. SUMMARY AND CONCLUSIONS

In conclusion, we found a striking correlation of  $R$  and  $m$ , revealed in Fig. 2(a). The canonical explanation for  $R > 1$  assumes that the number of order parameters involved in the glass transition is larger than one [46–49,53]. However, the observed scaling of the PDR with fragility is in favor of an alternative interpretation: The deviations of  $R$  from unity are related to the separation of the kinetic glass transition from a hidden phase transition into an ideal equilibrium glass. For fragile glass formers,  $T_g$  comes close to the ideal glass-transition temperature, approximated by  $T_{VF}$  [Fig. 1(b)]. Hence, for such systems the measurements of the thermodynamic and mechanical quantities at  $T_g$ , entering the PDR, are in fact performed at a temperature close to the phase transition into the equilibrium glass. Then it seems plausible that the anomalies at  $T_g$  (just as the value of  $T_g$  itself) are not too far off the corresponding values at the (dynamically inaccessible) ideal glass transition. Therefore, in these cases  $R$  approaches unity, as predicted by the Ehrenfest relations for second-order phase transitions. In contrast, for strong systems the relevant quantities measured at  $T_g \gg T_{VF}$  are collected at a temperature far above the transition into the equilibrium glass. In this situation, the Ehrenfest relations cannot be valid, resulting in a PDR significantly larger than unity. Overall, considering the scenario discussed above, the  $R(m)$  scaling discovered in the present work is well consistent with models assuming that glassy freezing is connected to a hidden, underlying phase transition. This is essentially based on the assumption that the PDR should approach unity when the glass transition comes successively closer to a true critical point. While this seems plausible, a theoretical foundation of this notion would be desirable. In any case, we think the explanation of the found  $R(m)$  scaling represents an important benchmark for any existing models of the glass transition and will hopefully stimulate new theoretical developments.

#### APPENDIX A: CRITICAL DISCUSSION OF THE VOGEL-FULCHER-TAMMANN LAW AND ON THE ASSUMPTION $T_K \sim T_{VF}$

The Vogel-Fulcher-Tammann (VFT) law, considered in the main text, is commonly used to describe the super-Arrhenius behavior of mean relaxation times or of viscosity in a broad range of temperatures and frequencies. It exhibits an extrapolated critical temperature below glassy freezing, where the relaxation times would diverge. As mentioned in the main text, it has been documented experimentally that this Vogel-Fulcher temperature  $T_{VF}$  is very close to the Kauzmann temperature [5,37,38] where the extrapolated entropy of the supercooled liquid falls below the entropy of the fully ordered crystal, which, according to popular wisdom, could indicate a phase transition into an ideal low-temperature glass phase. However, there seem to exist glass-forming materials, specifically strong liquids, where this strict correlation  $T_K \approx T_{VF}$  can be violated [69]. Deviations in the ratio  $T_K/T_{VF}$  were found by Tanaka *et al.* [69] for some metallic glasses

( $T_K/T_{VF} = 1.3-1.5$ ) and for some network glasses ( $\text{SiO}_2$ :  $T_K/T_{VF} = 1.7$  and  $\text{GeO}_2$ :  $T_K/T_{VF} = 2.1$ ). For all the other systems this ratio is close to unity, as is assumed in the present work. First, in strong glasses both characteristic temperatures are far below the kinetic glass transition, and they depend strongly on extrapolation resulting in large uncertainties. Second, even if these temperatures would be correct, and if a hidden phase transition happens at  $T_K$  rather than at  $T_{VF}$ , this would not change our reasoning considerably. Even assuming a factor of 2 for the ratio of these characteristic temperatures for strong glasses still results in a continuous increase of  $T_g/T_K$  towards low fragilities.

Notably, the VFT law is not the only possibility to parametrize the super-Arrhenius behavior of relaxation times. For example, there are proposals by Mauro *et al.* [20] or Krausser *et al.* [22] that work equally well [35,36] with a similar number of parameters, but without introducing a finite critical temperature. In the Krausser-Samwer-Zaccone model [22], a universal correlation between the repulsive steepness parameter  $\lambda$  of the interparticle potential and the liquid fragility  $m$  was found, which finally has been proven utilizing broadband dielectric spectroscopy [36].

We are aware of critical concerns regarding the use of one single VFT law, or simple extrapolations to low temperatures, as documented in Fig. 1(a) of the main text. In particular, we refer to Stickel *et al.* [70,71], who reported anomalies in the variation of the relaxation times at characteristic temperatures. However, with reference to the extensive broadband dielectric spectroscopy work, including very-low frequency and aging data, as published by Lunkenheimer, Loidl, and co-workers [72–75], it seems fair to say that the VFT law, according to Occam’s razor, is the most reasonable ansatz to describe broadband relaxation data and finally is a widely accepted ansatz in the glass community.

To document the validity of the fit parameters obtained by describing super-Arrhenius behavior of relaxational dynamics using the VFT law, in Fig. 3 we show two illuminating examples: relaxation times from broadband dielectric spectroscopy (BDS) data of glycerol, where the VFT fits work rather well in the complete range of measured relaxation times (left frame), and corresponding data of propylene carbonate (PC), where the VFT law significantly deviates, especially at low relaxation times (right frame). Figure 3 illustrates how VF temperatures may change depending on fit ranges.

The blue lines in both frames are VFT fits including all data points measured in the complete time/temperature regime. The fit certainly works well in glycerol, with minor deviations at the shortest times. In PC at the shortest times/highest temperatures, stronger deviations become apparent, possibly indicative for some type of crossover temperature, which will not be discussed here in detail. Fits utilizing restricted temperature regimes, specifically neglecting high-temperature data, are shown by red and green lines. As indicated in the figure legends, we find that the resulting VF temperatures are only moderately changed, with a variation in the percent range. Resulting deviations in the fragility indices, determined from the VFT parameters, are more significant and, in PC, reach up to 25%. It is a general observation that VF temperatures are rather well defined, while for the fragility index rather large error bars must be assumed.

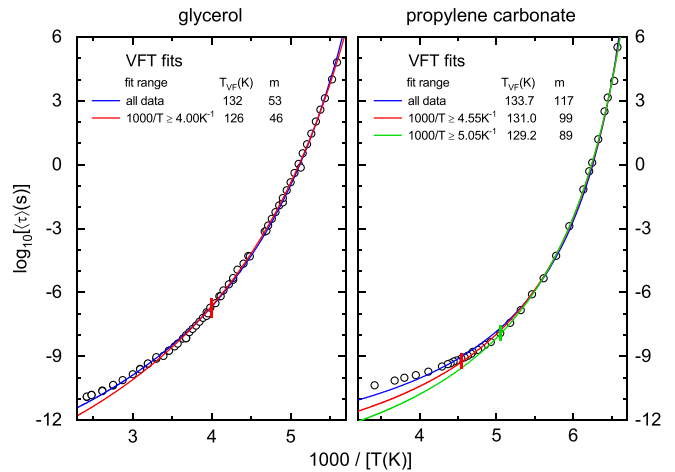


FIG. 3. Temperature dependence of relaxation times from BDS measurements in the supercooled liquids glycerol and propylene carbonate in Arrhenius representation. For comparison, fits covering different temperature regimes as indicated in the figures are shown (the vertical bars indicate the high-temperature limits of these regimes). The resulting VF temperatures and fragilities are listed in the figure legends and discussed in the text. The  $\tau(T)$  data were taken from Refs. [35,76].

Finally, it seems important to mention that both data sets cover more than 15 decades of time/frequency, starting at very short times close to the inverse attempt frequencies up to very long times, significantly exceeding the glass-transition temperature. All data were measured in thermodynamic equilibrium, including the long-time data, which were derived from aging experiments [76]. Even of higher relevance is the fact that the super-Arrhenius behavior is strictly valid far beyond the glass-transition temperature. These results are in good agreement with MC simulations of Berthier and co-workers [28,29] of relaxation times and configurational entropies utilizing the SWAP algorithm, which were calculated significantly below the glass-transition temperature and by experiments on ultrastable glasses [30] showing that the Kauzmann temperature remains a valid and useful hypothesis to interpret glass formation.

## APPENDIX B: GLASS-TRANSITION PHENOMENA

As mentioned in the main text, the glass transition is a kinetic phenomenon, indicating the cross-over temperature when the system falls out of thermodynamic equilibrium, hence it depends on the cooling rate. Figure 4 schematically shows the main characteristics of glassy freezing according to textbook knowledge, using the temperature dependence of the volume as an instructive example. A crystalline material melts in a first-order phase transition at the melting temperature  $T_m$  with the appearance of considerable latent heat. If crystallization of a liquid can be avoided upon cooling, first a supercooled liquid forms, which finally, at a temperature  $T_g \approx 2/3T_m$ , undergoes glassy freezing. However, as outlined before, the glass transition is a kinetic phenomenon, and it depends on the cooling rate  $q$ , yielding lower transition temperatures for slower cooling. In the solid phases, glassy or crystalline, thermal expansion is governed by vibrational

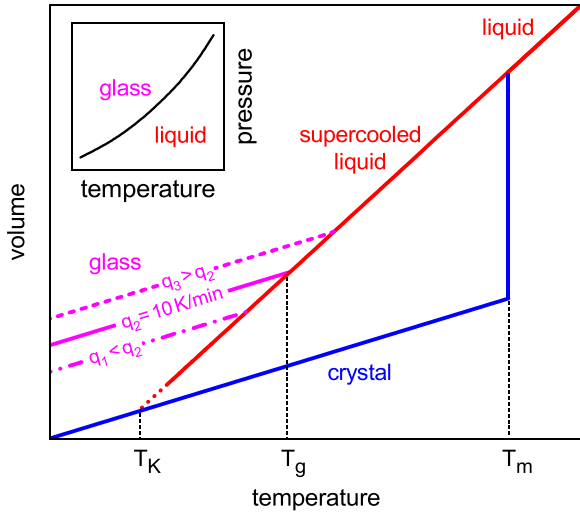


FIG. 4. Red line: Schematic temperature dependence of the volume  $V$  in the liquid and supercooled-liquid states above the glass transition. The behavior in the glass state is indicated by the magenta lines for three different cooling rates  $q_1 < q_2 < q_3$ . The canonically defined  $T_g$  marks the glass transition for a cooling rate  $q_2 \approx 10$  K/min. Blue line:  $V(T)$  in the crystalline state with melting temperature  $T_m$ .  $T_K$  indicates the Kauzmann temperature, which, in this plot, can be estimated from the extrapolated crossing of the supercooled-liquid and crystal  $V(T)$  traces. Inset: Schematic second-order ( $p, T$ ) phase diagram between a liquid and an ideal glass, ignoring kinetic phenomena. At the phase boundary, volume  $V$  and entropy  $S$  of the two phases are identical. The tentative thermodynamic phase transition is hidden by kinetic phenomena and is expected at lower temperatures, close to  $T_K$ .

contributions only, and it is similar for both solid modifications. In the supercooled-liquid phase, configurational contributions enhance the temperature dependence of the volume. On further cooling below  $T_g$ , assuming a constant thermal expansion, the glass finally would become denser than the crystal, roughly defining a critical temperature. Considering the excess entropy derived from specific-heat measurements, such a critical temperature was calculated by Kauzmann [25].

The inset of Fig. 4 shows a schematic ( $p, T$ ) phase diagram (with  $p$  being the external pressure) for a second-order phase-transition scenario, the line indicating a continuous transition from the liquid into the ideal glass. The first derivatives of free energy, entropy  $S$ , and volume  $V$  are continuous across the transition, i.e., they are identical just below and above the phase boundary, while the second derivatives of the Gibbs free energy, specific heat  $c_p$ , thermal expansion  $\alpha_p$ , and isothermal compressibility  $\kappa_T$  are discontinuous. In this schematic phase diagram, all kinetic phenomena are excluded, but they could be visualized by a broadening or smearing out of the phase boundary. At the glass transition and in continuous second-order phase transitions, latent heat contributions are completely absent.

#### APPENDIX C: REVIEW OF PUBLISHED DATA RELEVANT FOR THE RATIO $T_g/T_{VF}$

In Fig. 1(b) of the main manuscript, we show the fragility dependence of the ratio  $T_g/T_{VF}$ . Here the theoretical

predictions are compared to experimental results where the involved quantities were deduced from  $\tau(T)$  or  $\eta(T)$  data. In Table I, we summarize all the published values of fragility, glass-transition temperature  $T_g$ , and Vogel-Fulcher temperature  $T_{VF}$  for a variety of supercooled liquids as documented in Fig. 1(b). Here we show the available data for polymers, molecular, ionic, and metallic glass formers, as well as for network silicates and other network-forming systems. Notably, some of the values on ion conductors were derived from dielectric modulus or conductivity spectra. All references are given directly in the table. In Tables I and II, we partly refer to a recent work by Lunkenheimer *et al.* [66] presenting a critical survey of existing literature data on glass-transition temperatures, fragilities, and thermal expansivities of various supercooled liquids and glasses.

#### APPENDIX D: CRITICAL REVIEW OF PUBLISHED DATA ON GLASS-FORMING LIQUIDS RELEVANT FOR THE PRIGOGINE-DEFAY RATIO

In Table II we provide the relevant data for a variety of glass-forming materials, namely for systems where heat capacity, thermal expansion, and compressibility were measured above and below the glass transition, and fragilities have been determined. In addition, the glass-transition temperature  $T_g$  and the volume at the transition  $V_g$  are indicated. From these quantities, the Prigogine-Defay ratio  $R$  can be directly calculated (last column). All quantities are given in SI units, and references are included directly in the table. As mentioned in the main text, we always try to refer to the original literature providing the experimental results, and in the case of multiple experiments we adapted the best documented results. By this wording we denote data from publications that provide appropriate figures with a detailed analysis of the measurements, so that the experienced reader can judge the quality of the result. This will be detailed later.

Table II documents that most of the listed polymers—polyvinyl chloride (PVC), polystyrene (PS), polypropylene (PP), polycarbonate (PC), polyarylate (PA), phenoxy (PH), polysulfone (PSF), and polyvinyl acetate (PVA)—have relatively large  $m$  values as generally found in polymers. Exceptions are polyisobutylene (PIB) and polyethylene (PE) with significantly lower fragilities. Table II also includes the van der Waals bonded, small organic-molecule system o-terphenyl (OTP) and results for OTP-OPP (o-terphenyl with o-phenylphenol) mixtures. In addition, it shows data for various hydrogen-bonded liquids, like *n*-propanol and glycerol, as well as for several inorganic covalent network-forming liquids, like amorphous selenium (Se), and some oxides, like  $B_2O_3$ ,  $GeO_2$ , the silicate glass  $26Na_2O-74SiO_2$ , albite ( $NaAlSi_3O_8$ ), and amorphous silica  $SiO_2$ . The latter all reveal rather low fragilities, with  $SiO_2$  and  $GeO_2$  belonging to the strongest supercooled liquids known. We also added the ionic melt  $2Ca(NO_3)_2 : 3KNO_3$  (CKN), which is an ionic mixed system close to the eutectic point and the metallic glass  $Zr_{46.75}Ti_{8.25}Cu_{7.5}Ni_{10}Be_{27.5}$  (ZrTiCuNiBe). In Ref. [113] erroneously a Zr percentage of 46.25 instead of 46.75 was specified. In addition, the values for the metallic glass, given in Table II, mostly refer to the similar compound  $Zr_{41.2}Ti_{13.8}Cu_{12.5}Ni_{10}Be_{22.5}$  [113]. Our slightly different  $R$

TABLE I. Data used for constructing Fig. 1(b) to document the significant fragility dependence of the ratio  $T_g/T_{VF}$ : Fragility  $m$ , glass-transition temperature  $T_g$ , and Vogel-Fulcher temperature  $T_{VF}$  of various glass formers plotted in Fig. 1(b).

	$m$	$T_g$ (K)	$T_{VF}$ (K)
<b>Polymers:</b>			
Polyisobutylene (PIB)	46 [66]	195 [66]	142 [77]
Poly( <i>n</i> -butyl methacrylate)	75 [66]	293 [66]	250 [78]
Poly(ethyl methacrylate)	81 [66]	338 [66]	275 [78]
Poly(ethylene oxide): LiTFSI	90 [79]	219 [79]	177 [79]
Polyvinyl acetate (PVA)	95 [66]	304 [66]	250 [80]
Poly(ethylene oxide)	132 [81]	219 [82]	184 [81]
Polycarbonate (PC)	132 [66]	415 [66]	371 [83]
Polypropylene (PP)	137 [84]	244 [85]	198 [77]
Polystyrene (PS)	139 [66]	365 [66]	322 [86]
Polysulfone (PSF)	141 [84]	459 [87]	414 [88]
Poly(methyl methacrylate)	145 [66]	378 [66]	318 [78]
Phenoxy (PH)	168 [88]	341.2 [87]	311 [88]
Polyvinyl chloride (PVC)	191 [66]	355 [66]	330 [89]
Polyarylate (PA)	218 [88]	450 [87]	415 [88]
<b>Molecular:</b>			
Propylene glycol	52 [66]	168 [66]	115 [35]
Ethanol	52 [66]	99 [66]	76.5 [35]
Glycerol	53 [66]	185 [66]	132 [35]
$\alpha\alpha\beta$ -tris-naphthylbenzene (TNB)	66 [66]	342 [66]	248 [90]
Dipropylene glycol	69 [91]	193 [35]	149 [35]
Salol	73 [62]	218 [62]	182 [35]
Tripropylene glycol	74 [91]	189 [35]	151 [35]
Glucose	79 [66]	305 [66]	242 [92]
OTP	81 [66]	245 [66]	193 [90]
Xylitol	86 [66]	248 [66]	207 [35]
Sorbitol	93 [66]	274 [66]	233 [35]
Propylene carbonate	104 [66]	159 [66]	134 [35]
Benzophenone	125 [93]	212 [94]	191 [35]
<b>Ionic:</b>			
Glyceline	47 [95]	175 [95]	113 [95]
Reline	57 [95]	205 [95]	152 [95]
Ethaline	60 [95]	155 [95]	113 [95]
Benzmim Cl	78 [96]	253 [96]	202 [96]
Omim PF <sub>6</sub>	78 [66]	194 [66]	153 [96]
Bmim BF <sub>4</sub>	93 [66]	182 [66]	149 [96]
2Ca(NO <sub>3</sub> ) <sub>2</sub> :3KNO <sub>3</sub> (CKN)	93 [66]	333 [66]	273 [35]
Bmim Cl	97 [66]	228 [66]	190 [96]
2Ca(NO <sub>3</sub> ) <sub>2</sub> :3RbNO <sub>3</sub>	141 [35]	333 [97]	285 [35]
Bmim FeCl <sub>4</sub>	144 [66]	182 [66]	159 [96]
[Li + DiMim]TFSI	145 [96]	202 [96]	180 [96]
Bmim FeCl <sub>3</sub> Br	146 [96]	180 [96]	159 [96]
Emim TCM	158 [96]	183 [96]	163 [96]
<b>Metallic:</b>			
Zr <sub>41.2</sub> Ti <sub>13.8</sub> Cu <sub>12.5</sub> Ni <sub>10</sub> Be <sub>22.5</sub>	39 [66]	625 [66]	387 [98]
Zr <sub>46.75</sub> Ti <sub>8.25</sub> Cu <sub>7.5</sub> Ni <sub>10</sub> Be <sub>27.5</sub>	43 [98]	597 [98]	376 [98]
Mg <sub>65</sub> Cu <sub>25</sub> Y <sub>10</sub>	45 [66]	380 [66]	261 [98]
Zr <sub>58.5</sub> Cu <sub>15.6</sub> Ni <sub>12.8</sub> Al <sub>10.3</sub> Nb <sub>2.8</sub>	46 [98]	666 [98]	437 [98]
Zr <sub>11</sub> Cu <sub>47</sub> Ti <sub>34</sub> Ni <sub>8</sub>	47 [66]	658 [66]	427 [98]
Pt <sub>45</sub> Ni <sub>30</sub> P <sub>25</sub>	48 [99]	496 [66]	320 [99]
Pd <sub>40</sub> Ni <sub>40</sub> P <sub>20</sub>	50 [66]	569 [66]	396 [98]
Pt <sub>57.3</sub> Cu <sub>14.6</sub> Ni <sub>5.3</sub> P <sub>22.8</sub>	52 [98]	482 [98]	336 [98]

TABLE I. (Continued.)

	$m$	$T_g$ (K)	$T_{VF}$ (K)
Pd <sub>40</sub> Cu <sub>30</sub> Ni <sub>10</sub> P <sub>20</sub>	57 [98]	578 [98]	418 [98]
Pd <sub>43</sub> Cu <sub>27</sub> Ni <sub>10</sub> P <sub>20</sub>	73 [98]	568 [98]	446 [98]
<b>Network silicates:</b>			
SiO <sub>2</sub>	20 [66]	1446 [66]	185 [100]
Albite	22 [66]	922 [66]	371 [101]
Cordierite	25 [102]	1096 [66]	451 [102]
80SiO <sub>2</sub> :20Na <sub>2</sub> O mol%	37 [66]	770 [66]	427 [90]
Na <sub>2</sub> Si <sub>2</sub> O <sub>5</sub>	45 [66]	713 [66]	501 [100]
Diopside	53 [66]	1013 [66]	718 [90]
Anorthite	54 [66]	1111 [66]	776 [90]
<b>Other network systems:</b>			
GeO <sub>2</sub>	20 [66]	787 [66]	233 [90]
ZnCl <sub>2</sub>	30 [66]	380 [66]	311 [100]
B <sub>2</sub> O <sub>3</sub>	32 [66]	554 [66]	352 [90]
60Se:40As mol%	36 [66]	445 [66]	335 [103]
S	86 [66]	246 [66]	224 [104]
Se	87 [66]	310 [66]	284 [105]

value, as compared to Ref. [113], results from the fact that we used the calorimetric glass-transition temperature. Already a rough inspection of Table II reveals that the polymers mainly exhibit high fragilities and Prigogine-Defay ratios between 1 and 2, while the glass formers with low fragility tend to have significantly higher  $R$  values.

As stated above, we tried to provide a neutral and as objective as possible treatment of all published data. By no means have we chosen values fitting better into the found correlation. As an example, we mention the PDR of PS. We preferred to take the incremental specific-heat values published by Takahara *et al.* [106], relying on a very precise calorimetric method, yielding  $R = 1.7$ , even though the PDR ( $R = 1.4$ ) as determined by Oels and Rehage [122] in a very detailed study of all incremental thermodynamic quantities entering the PDR of PS would fit even better into the found dependence. By comparison with other published tables on the PDR, we further want to elucidate our choice of the most reliable published data. A similar but less comprehensive table than Table II has been published by Donth [50]. While most of the data shown there are well within the scatter as documented in Fig. 2(a), glycerol with  $R = 9.4$  is a notable exception compared to  $R = 3.6$  documented in Table II. This significant discrepancy results from the incremental value of the thermal expansion, where Donth [50] relies on a result determined by ultrasound techniques, while later certainly more precise values have been determined (see, e.g., Ref. [110]). This statement is in accord with comments provided in the Supplemental Materials of Refs. [65] and [66]. Some characteristic PDR values were also published in the work of Schmelzer and Guzkow [57]. However, most of the references given there refer to published review articles, which partly even refer to further reviews, like that of Davies and Jones [47], where the PDR values are not documented in detail and even the authors themselves make critical comments about the reliability of the data.

TABLE II. Glass-transition temperature  $T_g$ , fragility  $m$ , and volume  $V_g$  at  $T_g$ .  $\Delta\alpha_p$ ,  $\Delta c_p$ , and  $\Delta\kappa_T$  denote incremental variations of thermal volume expansion, heat capacity, and isothermal compressibility at the glass-transition temperature. All quantities are given in SI units. The resulting PDR  $R$  is presented in the last column. The relevant references are given in the table. These values were used to calculate the fragility dependence of the PDR, as well as the fragility dependence of the Ehrenfest equations.

	$T_g$ (K)	$m$	$10^3 V_g$ (m <sup>3</sup> /kg)	$10^4 \Delta\alpha_p$ (K <sup>-1</sup> )	$10^{-2} \Delta c_p$ J/(kg K)	$10^{12} \Delta\kappa_T$ (m <sup>2</sup> /N)	$R$
PVC	355 [66]	191 <sup>a</sup> [66]	0.73 [85]	3.1 [66]	3.0 [85]	200 [85]	2.4
PS	365 [66]	139 [66]	0.968 [106]	2.97 [66]	3.27 [87]	160 [87]	1.7
PP	244 [85]	137 [84]	1.13 [85]	4.4 [85]	4.8 [85]	90 [85]	0.81
PC	415 [66]	132 [66]	0.863 [87]	3.44 [66]	2.3 [87]	192 [87]	1.05
PA	450 [87]	218 <sup>a</sup> [88]	0.8544 [87]	3.59 [87]	2.28 [87]	202 [87]	0.93
PH	341.2 [87]	168 [88]	0.8621 [87]	3.30 [87]	4.23 [87]	88.7 [87]	1.17
PSF	459.0 [87]	141 [84]	0.8374 [87]	3.55 [87]	2.26 [87]	204 [87]	0.95
PVA	304 [66]	95 [66]	0.843 [52]	4.3 [66]	5.0 [52]	208.5 [52]	2.2
PIB	195 [66]	46 [66]	1.05 [85]	3.75 [107]	4.0 [85]	100 [85]	1.4
PE	237 [84]	46 [84]	1.04 [85]	3.14 [107]	6.0 [85]	200 [85]	4.9
OTP	245 [66]	81 [66]	0.894 [108]	4.76 [66]	4.71 [108]	114 [108]	1.1
OTP-OPP	234 [66]	72 [109]	0.969 [106]	6.0 [66]	5.84 [106]	150 [106]	1.1
<i>n</i> -propanol	96 [66]	77 [100]	0.915 [85]	4.0 [85]	6.7 [85]	40 [85]	1.9
Glucose	305 [66]	79 [66]	0.649 [85]	2.57 [66]	7.53 [85]	61 [85]	3.5
Glycerol	185 [66]	53 [66]	0.752 [110]	4.0 [66]	9.8 [111]	81 [112]	3.6
CKN	333 [66]	93 [66]	0.456 [52]	2.44 [66]	5.4 [52]	69 [52]	4.1
ZrTiCuNiBe	625 [66]	39 [66]	0.164 [113]	0.193 [66]	7.03 [113]	0.0785 [113]	1.4
Se	310 [66]	87 [66]	0.2339 [114]	2.2 [66]	1.82 [115]	37 [114]	1.9
B <sub>2</sub> O <sub>3</sub>	554 [66]	32 [66]	0.558 [52]	2.77 [66]	6.3 [52]	280 [52]	7.4
GeO <sub>2</sub>	787 [66]	20 [66]	0.278 [116]	0.36 [66]	0.53 [116]	81.9 [116]	15
26Na <sub>2</sub> O–74SiO <sub>2</sub>	735 [117]	30 [84]	0.418 [117]	0.7 [117]	2.36 [117]	30 [117]	4.7
Albite	922 [66]	22 [66]	0.426 <sup>b</sup> [118]	0.31 [66]	1.22 [116]	30 <sup>c</sup> [116]	9.7
SiO <sub>2</sub>	1446 [66]	20 [66]	0.454 [116]	0.036 <sup>d</sup> [66]	0.033 [119]	56.9 [116]	22.1

<sup>a</sup>An upper limit of liquid fragility values was provided by Böhmer *et al.* [62] with  $m < 200$ . Probably more realistic maximum values for nonpolymeric supercooled liquids were provided by Wang and Mauro [120] with  $m < 175$  and by Wang *et al.* [121] with  $m < 170$ . According to these references, we believe that the fragilities cited in this table, including polymers, ranging from values of 20 to 218, are certainly realistic.

<sup>b</sup>Volume calculated from Ref. [118], assuming the values at  $T_g$  of albite synthesized with technical grade chemicals. Effective lifetime not corrected for feeding.

<sup>c</sup>This value taken from Ref. [116] reveals large uncertainty. Here we took the mean value.

<sup>d</sup>No reliable values for the thermal expansivity in the supercooled liquid are available in the literature. We took a value of  $\alpha_1 = 3\alpha_g$  following a rule of thumb as given in Ref. [66]. See the detailed discussion in Appendix D.

In addition, some comments are necessary here regarding the PDR value of amorphous silica. So far, no reliable PDR was published for this compound, mainly because the jumps in heat capacity and thermal expansion are not well documented. In the literature,  $R$  values of SiO<sub>2</sub> range between  $10^3$  and  $10^5$  [64,65]. By analyzing the heat-capacity jump at  $T_g$  from Ref. [119] and assuming that the thermal expansion in the supercooled liquid is three times that of the glass [66], we arrive at  $R \approx 22.1$ , which is reliable when compared to values reported for other oxides. Notably, this value seems to be consistent with published  $R$  values of sodium- and potassium-doped SiO<sub>2</sub> [64]. For all compounds studied there, the  $R$  values strongly increase upon decreasing doping, and for the lowest doping levels of  $\sim 10$  mol% Na<sub>2</sub>O or K<sub>2</sub>O in SiO<sub>2</sub> the PDR values range between  $13 < R < 16$ , which fits well into our found correlation documented in Fig. 2(a).

#### APPENDIX E: UNCERTAINTIES OF THE PDR VALUES AND REMARKS ON THE SCATTER OF DATA IN THEIR FRAGILITY DEPENDENCE

We are aware that there is significant scatter of data in the fragility dependence of  $R$  [Fig. 2(a)]. The question arises if the found correlation  $R(m)$  is significant. This is an important question as it raises serious doubts about the canonical interpretation that deviations from  $R = 1$  can be rationalized considering more than one order parameter [47]. It is almost impossible to provide a realistic estimate of error bars for the PDR shown in Fig. 2(a). In the original literature, in most cases no error bars are provided for the incremental values listed in Table II. In addition, the same quantities often were determined using different experimental techniques, with varying temperature ranges for the evaluation of the data for  $T < T_g$  and  $T > T_g$ . Furthermore, as outlined in the main text (Sec. I B), minor effects may result from varying cooling



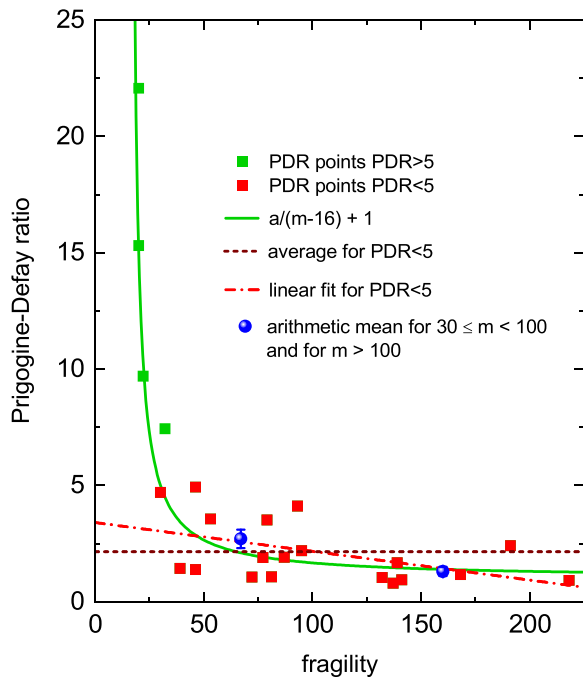


FIG. 5. Statistical analysis of the scatter of PDR values plotted in Fig. 2(a) and documented in Table II. The PDR values are grouped according to  $PDR > 5$  (green squares) and  $PDR < 5$  (red squares) (see the text). A linear fit for  $PDR < 5$  is shown as a red dash-dotted line. The two blue spheres indicate the arithmetic means for data groups ( $30 \leq m < 100$ ) and for  $m > 100$ . The solid green line is a fit using the proposed  $R(m)$  correlation for all documented PDR values, as also shown in Fig. 2(a).

rates and a different history dependence. From our point of view, the scatter of data as documented in Fig. 2 provides the most realistic measure of uncertainties of the PDR. The significance of our interpretation and a more detailed analysis of the scatter of PDR data documented in Fig. 2(a) are outlined in the following.

During the reviewing process of this work, the proposal was made to neglect the  $R$  values of all strong liquids ( $R > 5$ ) and to only analyze the remaining data points. These data scatter between  $1 < R < 5$ , values that are commonly considered for the PDR of supercooled liquids. To document the significance of our data, in Fig. 5 we replot the data shown in Fig. 2(a) and listed in Table II on a linear scale. The average of the data points with  $R < 5$  (red squares) gives  $R = 2.15$  (brown dashed line). However, already a first inspection documents that the deviations from this mean value are significantly different for fragilities  $m < 100$  and  $m > 100$ . The arithmetic means including the standard deviations for these two regimes are indicated as blue spheres with error bars in Fig. 5. They are clearly above (for  $m < 100$ ) and below ( $m > 100$ ) the average value of 2.15. In addition, a least-squares fit of all data with  $R < 5$  (red dash-dotted line) reveals a significant negative slope  $\neq 0$  and is in good agreement with the mean values of the two regimes (blue points). Summarizing, Fig. 5 provides good arguments for a decrease of the PDR with increasing  $m$  of supercooled liquids even when taking intermediate and fragile glasses into account only. In addition, the  $R$  values continuously increase for decreasing fragilities from the most fragile to the strongest glasses without any significant discontinuity. There is no evident reason to ignore the values for strong glass formers ( $R > 5$ ).

- [1] M. D. Ediger, C. A. Angell, and S. R. Nagel, Supercooled liquids and glasses, *J. Phys. Chem.* **100**, 13200 (1996).
- [2] P. G. Debenedetti and F. H. Stillinger, Supercooled liquids and the glass transition, *Nature (London)* **410**, 259 (2001).
- [3] C. A. Angell, Formation of glasses from liquids and biopolymers, *Science* **267**, 1924 (2005).
- [4] J. C. Dyre, Colloquium: The glass transition and elastic models of glass-forming liquids, *Rev. Mod. Phys.* **78**, 953 (2006).
- [5] L. Berthier and G. Biroli, Theoretical perspective on the glass transition and amorphous materials, *Rev. Mod. Phys.* **83**, 587 (2011).
- [6] M. D. Ediger and P. Harrowell, Perspective: Supercooled liquids and glasses, *J. Chem. Phys.* **137**, 080901 (2012).
- [7] L. Berthier and D. L. Reichmann, Modern computational studies of the glass transition, *Nat. Rev. Phys.* **5**, 102 (2023).
- [8] K. L. Ngai, Universal properties of relaxation and diffusion in complex materials: Originating from fundamental physics with rich applications, *Prog. Mat. Sci.* **139**, 101130 (2023).
- [9] J. H. Gibbs and E. A. DiMarzio, Nature of the glass transition and the glassy state, *J. Chem. Phys.* **28**, 373 (1958).
- [10] G. Adam and J. H. Gibbs, On the temperature dependence of cooperative relaxation properties in glass-forming liquids, *J. Chem. Phys.* **43**, 139 (1965).
- [11] T. R. Kirkpatrick and P. G. Wolynes, Connections between some kinetic and equilibrium theories of the glass transition, *Phys. Rev. A* **35**, 3072 (1987).
- [12] T. R. Kirkpatrick, D. Thirumalai, and P. G. Wolynes, Scaling concepts for the dynamics of viscous liquids near an ideal glassy state, *Phys. Rev. A* **40**, 1045 (1989).
- [13] M. H. Cohen and D. Turnbull, Molecular transport in liquids and glasses, *J. Chem. Phys.* **31**, 1164 (1959).
- [14] G. S. Grest and M. H. Cohen, Liquids, glasses, and the glass transition: A free-volume approach, in *Advances in Chemical Physics*, edited by I. Prigogine, and S. A. Rice (Wiley, New York, 1981), Vol. 48, pp. 455–525.
- [15] E. Leutheusser, Dynamical model of the liquid-glass transition, *Phys. Rev. A* **29**, 2765 (1984).
- [16] U. Bengtzelius, W. Götze, and A. Sjölander, Dynamics of supercooled liquids and the glass transition, *J. Phys. C* **17**, 5915 (1984).
- [17] W. Götze and L. Sjögren, Relaxation processes in supercooled liquids, *Rep. Prog. Phys.* **55**, 241 (1992).
- [18] D. Kivelson, S. A. Kivelson, X-L. Zhao, Z. Nussinov, and G. Tarjus, A thermodynamic theory of supercooled liquids, *Physica A* **219**, 27 (1995).
- [19] C. A. Angell and K. J. Rao, Configurational excitations in condensed matter, and the "Bond Lattice" model for the liquid-glass transition, *J. Chem. Phys.* **57**, 470 (1972).

- [20] J. C. Mauro, Y. Yue, A. J. Ellison, P. K. Gupta, and D. C. Allan, Viscosity of glass-forming liquids, *Proc. Natl. Acad. Sci. USA* **106**, 19780 (2009).
- [21] D. Chandler and J. P. Garrahan, Dynamics on the way to forming glass: Bubbles in space–time, *Annu. Rev. Phys. Chem.* **61**, 191 (2010).
- [22] J. Krausser, K. H. Samwer, and A. Zaccone, Interatomic repulsion softness directly controls the fragility of supercooled metallic melts, *Proc. Natl. Acad. Sci. USA* **112**, 13762 (2015).
- [23] Y. Shen, K. Samwer, W. L. Johnson, W. A. Goddard, and Q. An, Phase formation and phase stability for the homogeneous and heterogeneous amorphous metals versus the crystalline phase, *Proc. Natl. Acad. Sci. USA* **122**, e2404489122 (2025).
- [24] L. Gao, H.-B. Yu, T. B. Schröder, and J. C. Dyre, Unified percolation scenario for the  $\alpha$  and  $\beta$  processes in simple glass formers, *Nat. Phys.* **21**, 471 (2025).
- [25] W. Kauzmann, The nature of the glassy state and the behavior of liquids at low temperatures, *Chem. Rev.* **43**, 219 (1948).
- [26] F. H. Stillinger, Supercooled liquids, glass transitions, and the Kauzmann Paradox, *J. Chem. Phys.* **88**, 7818 (1988).
- [27] F. H. Stillinger, P. G. Debenedetti, and T. M. Truskett, The Kauzmann Paradox revisited, *J. Phys. Chem. B* **105**, 11809 (2001).
- [28] L. Berthier, M. Ozawa, and C. Scalliet, Configurational entropy of glass-forming liquids, *J. Chem. Phys.* **150**, 160902 (2019).
- [29] L. Berthier, G. Biroli, J.-P. Bouchaud, and G. Tarjus, Can the glass transition be explained without a growing static length scale? *J. Chem. Phys.* **150**, 094501 (2019).
- [30] M. S. Beasley, C. Bishop, B. J. Kasting, and M. D. Ediger, Vapor-deposited ethylbenzene glasses approach “ideal glass” density, *J. Phys. Chem. Lett.* **10**, 4069 (2019).
- [31] H. Vogel, Das Temperaturabhängigkeitsgesetz der Viskosität von Flüssigkeiten, *Phys. Z.* **22**, 645 (1921).
- [32] G. S. Fulcher, Analysis of recent measurements of the viscosity of glasses, *J. Am. Ceram. Soc.* **8**, 339 (1923).
- [33] G. Tammann and W. Hesse, Die Abhängigkeit der Viskosität von der Temperatur bei unterkühlten Flüssigkeiten, *Z. Anorg. Allg. Chem.* **156**, 245 (1926).
- [34] C. A. Angell, Strong and fragile liquids, in *Relaxations in Complex Systems*, edited by K. L. Ngai, and G. B. Wright (NRL, Washington, DC, 1985), p. 3.
- [35] P. Lunkenheimer, S. Kastner, M. Köhler, and A. Loidl, Temperature development of glassy  $\alpha$ -relaxation dynamics determined by broadband dielectric spectroscopy, *Phys. Rev. E* **81**, 051504 (2010).
- [36] P. Lunkenheimer, F. Humann, A. Loidl, and K. Samwer, Universal correlations between the fragility and interparticle repulsion of glass-forming liquids, *J. Chem. Phys.* **153**, 124507 (2020).
- [37] C. A. Angell, Relaxation in liquids, polymers and plastic crystals—strong/fragile patterns and problems, *J. Non-Cryst. Solids* **131-133**, 13 (1991).
- [38] R. Richert and C. A. Angell, Dynamics of glass-forming liquids. V. On the link between molecular dynamics and configurational entropy, *J. Chem. Phys.* **108**, 9016 (1998).
- [39] Th. Bauer, P. Lunkenheimer, and A. Loidl, Cooperativity and the freezing of molecular motion at the glass transition, *Phys. Rev. Lett.* **111**, 225702 (2013).
- [40] S. Franz and G. Parisi, On non-linear susceptibility in supercooled liquids, *J. Phys. Condens. Matter* **12**, 6335 (2000).
- [41] J.-P. Bouchaud and G. Biroli, Nonlinear susceptibility in glassy systems: A probe for cooperative dynamical length scales, *Phys. Rev. B* **72**, 064204 (2005).
- [42] C. Crauste-Thibierge, C. Brun, F. Ladieu, D. L’Hôte, G. Biroli, and J.-P. Bouchaud, Evidence of growing spatial correlations at the glass transition from nonlinear response experiments, *Phys. Rev. Lett.* **104**, 165703 (2010).
- [43] S. Albert, Th. Bauer, M. Michl, G. Biroli, J.-P. Bouchaud, A. Loidl, P. Lunkenheimer, R. Tourbot, C. Wiertel-Gasquet, and F. Ladieu, Fifth-order susceptibility unveils growth of thermodynamic amorphous order in glass-formers, *Science* **352**, 1308 (2016).
- [44] P. Ehrenfest, Phasenumwandlungen im ueblichen und erweiterten Sinn, classifiziert nach den entsprechenden Singularitaeten des thermodynamischen Potentiales, *Proc. R. Acad. Amsterdam* **36**, 153 (1933).
- [45] I. Prigogine and R. Defay, *Chemical thermodynamics* (Longman Greens, London, 1954).
- [46] R. O. Davies and G. O. Jones, The irreversible approach to equilibrium in glasses, *Proc. R. Soc. London Ser. A* **217**, 26 (1952).
- [47] R. O. Davies and G. O. Jones, Thermodynamic and kinetic properties of glasses, *Adv. Phys.* **2**, 370 (1953).
- [48] M. Goldstein, Some thermodynamic aspects of the glass transition: Free volume, entropy, and enthalpy theories, *J. Chem. Phys.* **39**, 3369 (1963).
- [49] J. O’Reilly, The effect of pressure on glass temperature and dielectric relaxation time of polyvinyl acetate, *J. Polym. Sci.* **57**, 429 (1962).
- [50] E. Donth, *The Glass Transition* (Springer, Berlin, 2001).
- [51] M. Goldstein, Viscous liquids and the glass transition. iv. thermodynamic equations and the transition, *J. Phys. Chem.* **77**, 667 (1973).
- [52] P. K. Gupta and C. T. Moynihan, Prigogine–Defay ratio for systems with more than one order parameter, *J. Chem. Phys.* **65**, 4136 (1976).
- [53] C. T. Moynihan and A. V. Lesikar, Comparison and analysis of relaxation processes at the glass transition temperature, *Ann. N.Y. Acad. Sci.* **371**, 151 (1981).
- [54] E. A. DiMarzio, Validity of the Ehrenfest relation for a system with more than one order parameter, *J. Appl. Phys.* **45**, 4143 (1974).
- [55] E. A. DiMarzio, Comments on a paper entitled “Prigogine–Defay ratio for systems with more than one order-parameter”, *J. Chem. Phys.* **67**, 2393 (1977).
- [56] Th. M. Nieuwenhuizen, Ehrenfest relations at the glass transition: Solution to an old paradox, *Phys. Rev. Lett.* **79**, 1317 (1997).
- [57] J. W. P. Schmelzer and I. Gutzow, The Prigogine-Defay ratio revisited, *J. Chem. Phys.* **125**, 184511 (2006).
- [58] T. V. Tropin, J. W. P. Schmelzer, I. Gutzow, and Ch. Schick, On the theoretical determination of the Prigogine-Defay ratio in glass transition, *J. Chem. Phys.* **136**, 124502 (2012).
- [59] N. L. Ellegaard, T. Christensen, P. V. Christiansen, N. B. Olsen, U. R. Pedersen, T. B. Schröder, and J. C. Dyre, Single-order-parameter description of glass-forming

- liquids: A one-frequency test, *J. Chem. Phys.* **126**, 074502 (2007).
- [60] K. Koperwas, A. Grzybowski, S. N. Tripathy, E. Masiewicz, and M. Paluch, Thermodynamic consequences of the kinetic nature of the glass transition, *Sci. Rep.* **5**, 17782 (2015).
- [61] G. B. McKenna, A brief discussion: Thermodynamic and dynamic fragilities, non-divergent dynamics and the Prigogine-Defay ratio, *J. Non-Cryst. Solids* **355**, 663 (2009).
- [62] R. Böhmer, K. L. Ngai, C. A. Angell, and D. J. Plazek, Non-exponential relaxations in strong and fragile glass formers, *J. Chem. Phys.* **99**, 4201 (1993).
- [63] A. Angell and W. Sichina, Thermodynamics of the glass transition: Empirical aspects, *Ann. N.Y. Acad. Sci.* **279**, 53 (1976).
- [64] S. V. Nemilov, *Thermodynamic and Kinetic Aspects of the Vitreous State* (CRC, London, 1994).
- [65] D. Gundermann, U. R. Pedersen, T. Hecksher, N. P. Bailey, B. Jakobsen, T. Christensen, N. B. Olsen, T. B. Schrøder, D. Fragiadakis, R. Casalini, C. M. Roland, J. C. Dyre, and K. Niss, Predicting the density-scaling exponent of a glass-forming liquid from Prigogine-Defay ratio measurements, *Nat. Phys.* **7**, 816 (2011).
- [66] P. Lunkenheimer, A. Loidl, B. Riechers, A. Zaccone, and K. Samwer, Thermal expansion and the glass transition, *Nat. Phys.* **19**, 694 (2023).
- [67] C. A. Angell, Glass formation and glass transition in supercooled liquids, with insights from study of related phenomena in crystals, *J. Non-Cryst. Solids* **354**, 4703 (2008).
- [68] C. A. Angell, Glass-formers and viscous liquid slow down since david turnbull: Enduring puzzles and new twists, *MRS Bull.* **33**, 545 (2005).
- [69] H. Tanaka, Relation between thermodynamics and kinetics of glass-forming liquids, *Phys. Rev. Lett.* **90**, 055701 (2003).
- [70] F. Stickel, E. W. Fischer, and R. Richert, Dynamics of glass-forming liquids. I. Temperature-derivative analysis of dielectric relaxation data, *J. Chem. Phys.* **102**, 6251 (1995).
- [71] F. Stickel, E. W. Fischer, and R. Richert, Dynamics of glass-forming liquids. II. Detailed comparison of dielectric relaxation, dc conductivity, and viscosity data, *J. Chem. Phys.* **104**, 2043 (1996).
- [72] P. Lunkenheimer, U. Schneider, R. Brand, and A. Loidl, Glassy dynamics, *Contemp. Phys.* **41**, 15 (2000).
- [73] P. Lunkenheimer and A. Loidl, Dielectric spectroscopy of glass-forming materials: A-relaxation and excess wing, *Chem. Phys.* **284**, 205 (2002).
- [74] P. Lunkenheimer, M. Köhler, S. Kastner, and A. Loidl, Dielectric spectroscopy of glassy dynamics, in *Structural Glasses and Supercooled Liquids*, edited by P. G. Wolynes, and V. Lubchenko (Wiley, Hoboken, NJ, 2012), pp. 115–149.
- [75] P. Lunkenheimer and A. Loidl, Glassy dynamics: From millihertz to terahertz, in *The Scaling of Relaxation Processes*, edited by F. Kremer, and A. Loidl (Springer, Cham, 2018), pp. 23–59.
- [76] P. Lunkenheimer, R. Wehn, U. Schneider, and A. Loidl, Glassy aging dynamics, *Phys. Rev. Lett.* **95**, 055702 (2005).
- [77] E. Krygier, G. X. Lin, J. Mendes, G. Mukandela, D. Azar, A. A. Jones, J. A. Pathak, R. H. Colby, S. K. Kumar, G. Floudas, R. Krishnamoorti, and R. Faust, Segmental dynamics of head-to-head polypropylene and polyisobutylene in their blend and pure components, *Macromolecules* **38**, 7721 (2005).
- [78] S. S. Teixeira, C. J. Dias, M. Dionisio, and L. C. Costa, New method to analyze dielectric relaxation processes: A study on polymethacrylate series, *Polym. Int.* **62**, 1744 (2013).
- [79] C. Do, P. Lunkenheimer, D. Diddens, M. Götz, M. Weiß, A. Loidl, X.-G. Sun, J. Allgaier, and M. Ohl, Li<sup>+</sup> transport in poly(ethylene oxide) based electrolytes: Neutron scattering, dielectric spectroscopy, and molecular dynamics simulations, *Phys. Rev. Lett.* **111**, 018301 (2013).
- [80] R. Richert, Scaling vs. Vogel-Fulcher-type structural relaxation in deeply supercooled materials, *Physica A* **287**, 26 (2000).
- [81] P. Lunkenheimer and A. Loidl, Relaxation dynamics of poly(ethylene oxide), [arXiv:2411.07807](https://arxiv.org/abs/2411.07807).
- [82] M. Schmidt and F. H. J. Maurer, Pressure-volume-temperature properties and free volume parameters of PEO/PMMA blends, *J. Polym. Sci. B* **36**, 1061 (1998).
- [83] P. A. O’Connell and G. B. McKenna, Arrhenius-type temperature dependence of the segmental relaxation below  $T_g$ , *J. Chem. Phys.* **110**, 11054 (1999).
- [84] D. Huang and G. B. McKenna, New insights into the fragility dilemma in liquids, *J. Chem. Phys.* **114**, 5621 (2001).
- [85] J. M. O’Reilly, Conformational specific heat of polymers, *J. Appl. Phys.* **48**, 4043 (1977).
- [86] A. Sahnoune, F. Massines, and L. Piché, Ultrasonic measurement of relaxation behavior in polystyrene, *J. Polym. Sci. B* **34**, 341 (1996).
- [87] P. Zoller, A study of the pressure-volume-temperature relationships of four related amorphous polymers: Polycarbonate, polyarylate, phenoxy, and polysulfone, *J. Polym. Sci.: Polym. Phys. Ed.* **20**, 1453 (1982).
- [88] E. Macho, A. Alegría, and J. Colmenero, Determining viscosity temperature behavior of four amorphous thermoplastics using a parallel plate technique, *Polym. Eng. Sci.* **27**, 810 (1987).
- [89] J. Colmenero, A. Arbe, and A. Alegría, The dynamics of the  $\alpha$ - and  $\beta$ -relaxations in glass-forming polymers studied by quasielastic neutron scattering and dielectric spectroscopy, *J. Non-Cryst. Solids* **172-174**, 126 (1994).
- [90] O. N. Senkov and D. B. Miracle, Description of the fragile behavior of glass-forming liquids with the use of experimentally accessible parameters, *J. Non-Cryst. Solids* **355**, 2596 (2009).
- [91] M. Köhler, P. Lunkenheimer, Y. Goncharov, R. Wehn, and A. Loidl, Glassy dynamics in mono-, di-, and tri-propylene glycol: From the  $\alpha$ - to the fast  $\beta$ -relaxation, *J. Non-Cryst. Solids* **356**, 529 (2010).
- [92] R. K. Chan, K. Pathmanathan, and G. P. Johari, Dielectric relaxations in the liquid and glassy states of glucose and its water mixtures, *J. Phys. Chem.* **90**, 6358 (1986).
- [93] P. Lunkenheimer, L. C. Pardo, M. Köhler, and A. Loidl, Broadband dielectric spectroscopy on benzophenone: A relaxation,  $\beta$  relaxation, and mode coupling theory, *Phys. Rev. E* **77**, 031506 (2008).
- [94] N. A. Davydova, V. I. Mel’nik, K. I. Nelipovitch, and J. Baran, Low-frequency Raman scattering from glassy and supercooled liquid benzophenone, *J. Mol. Struct.* **563-564**, 105 (2001).
- [95] D. Reuter, C. Binder, P. Lunkenheimer, and A. Loidl, Ionic conductivity of deep eutectic solvents: The role of

- orientational dynamics and glassy freezing, *Phys. Chem. Chem. Phys.* **21**, 6801 (2019).
- [96] P. Sippel, P. Lunkenheimer, S. Krohns, E. Thoms, and A. Loidl, Importance of liquid fragility for energy applications of ionic liquids, *Sci. Rep.* **5**, 13922 (2015).
- [97] A. Pimenov, P. Lunkenheimer, M. Nicklas, R. Böhmer, A. Loidl, and C. A. Angell, Ionic transport and heat capacity of glass-forming metal-nitrate mixtures, *J. Non-Cryst. Solids* **220**, 93 (1997).
- [98] I. Gallino, J. Schroers, and R. Busch, Kinetic and thermodynamic studies of the fragility of bulk metallic glass forming liquids, *J. Appl. Phys.* **108**, 063501 (2010).
- [99] H. S. Chen, A method for evaluating viscosities of metallic glasses from the rates of thermal transformations, *J. Non-Cryst. Solids* **27**, 257 (1978).
- [100] From the fits of  $\eta(T)$  of  $\text{SiO}_2$ ,  $\text{Na}_2\text{Si}_2\text{O}_5$ ,  $\text{ZnCl}_2$  and of  $\tau(T)$  of  $n$ -propanol, published in Ref. [36].
- [101] J. K. Russell and D. Giordano, A model for silicate melt viscosity in the system  $\text{CaMgSi}_2\text{O}_6$ - $\text{CaAl}_2\text{Si}_2\text{O}_8$ - $\text{NaAlSi}_3\text{O}_8$ , *Geochim. Cosmochim. Acta* **69**, 5333 (2005).
- [102] E. A. Giess, J. P. Fletcher, and L. W. Herron, Isothermal sintering of cordierite-type glass powders, *J. Am. Ceram. Soc.* **67**, 549 (1984).
- [103] D. W. Henderson and D. G. Ast, Viscosity and crystallization kinetics of  $\text{As}_2\text{Se}_3$ , *J. Non-Cryst. Solids* **64**, 43 (1984).
- [104] B. Ruta, G. Monaco, V. M. Giordano, F. Scarponi, D. Fioretto, G. Ruocco, K. S. Andrikopoulos, and S. N. Yannopoulos, Non-ergodicity factor, fragility, and elastic properties of polymeric glassy sulfur, *J. Phys. Chem. B* **115**, 14052 (2011).
- [105] D. J. Plazek and K. L. Ngai, The glass temperature, in *Physical Properties of Polymers Handbook*, edited by J. E. Mark (Springer, Berlin, 2007), Chap. 12.
- [106] S. Takahara, M. Ishikawa, O. Yamamuro, and T. Matsuo, Structural relaxations of glassy polystyrene and *o*-terphenyl studied by simultaneous measurement of enthalpy and volume under high pressure, *J. Phys. Chem. B* **103**, 792 (1999).
- [107] S. C. Sharma, L. Mandelkern, and F. C. Stehling, Relation between expansion coefficients and glass temperature, *Polym. Lett.* **10**, 345 (1972).
- [108] G. P. Johari, Prigogine-Defay ratio and its change with fictive temperature approaching the ideal glass transition, *Thermochim. Acta* **717**, 179343 (2022).
- [109] C. M. Roland, S. Capaccioli, M. Lucchesi, and R. Casalini, Adam-Gibbs model for the supercooled dynamics in the ortho-terphenyl ortho-phenylphenol mixture, *J. Chem. Phys.* **120**, 10640 (2004).
- [110] I. V. Blazhnov, N. P. Malomuzh, and S. V. Lishchuk, Temperature dependence of density, thermal expansion coefficient and shear viscosity of supercooled glycerol as a reflection of its structure, *J. Chem. Phys.* **121**, 6435 (2004).
- [111] L.-M. Wang, V. Velikov, and C. A. Angell, Direct determination of kinetic fragility indices of glassforming liquids by differential scanning calorimetry: Kinetic versus thermodynamic fragilities, *J. Chem. Phys.* **117**, 10184 (2002).
- [112] M. B. Tang, W. H. Wang, L. Xiac, and J. T. Zhao, Constant-volume heat capacity at glass transition, *J. Alloys Compounds* **577**, 299 (2013).
- [113] K. Samwer, R. Busch, and W. L. Johnson, Change of compressibility at the glass transition and Prigogine-Defay ratio in  $\text{ZrTiCuNiBe}$  alloys, *Phys. Rev. Lett.* **82**, 580 (1999).
- [114] J. I. Berg and R. Simha, Pressure-volume-temperature relations in liquid and glassy selenium, *J. Non-Cryst. Solids* **22**, 1 (1976).
- [115] M. Goldstein, Viscous liquids and the glass transition. V. Sources of the excess specific heat of the liquid, *J. Chem. Phys.* **64**, 4767 (1976).
- [116] D. B. Dingwell, R. Knoche, and S. L. Webb, A volume temperature relationship for liquid  $\text{GeO}_2$  and some geophysically relevant derived parameters for network liquids, *Phys. Chem. Miner.* **19**, 445 (1993).
- [117] L. Wondraczek and H. Behrens, Molar volume, excess enthalpy, and Prigogine-Defay ratio of some silicate glasses with different histories, *J. Chem. Phys.* **127**, 154403 (2007).
- [118] R. Knoche, D. B. Dingwell, and S. L. Webb, Non-linear temperature dependence of liquid volumes in the system albite-anorthite-diopside, *Contrib. Mineral. Petrol.* **111**, 61 (1992).
- [119] P. Richet and Y. Bottinga, Glass transitions and thermodynamic properties of amorphous  $\text{SiO}_2$ ,  $\text{NaAlSi}_n\text{O}_{2n+2}$  and  $\text{KAlSi}_3\text{O}_8$ , *Geochim. Cosmochim. Acta* **48**, 453 (1984).
- [120] L.-M. Wang and J. C. Mauro, An upper limit to kinetic fragility in glass-forming liquids, *J. Chem. Phys.* **134**, 044522 (2011).
- [121] L.-M. Wang, C. A. Angell, and R. Richert, Fragility and thermodynamics in nonpolymeric glass-forming liquids, *J. Chem. Phys.* **125**, 074505 (2006).
- [122] H.-J. Oels and G. Rehage, Pressure-volume-temperature measurements on atactic polystyrene. A thermodynamic view, *Macromolecules* **10**, 1036 (1977).